J Electroceram (2012) 29:204–210
DOI 10.1007/s10832-012-9763-y

Structural, dielectric and conductivity studies of $Na_2Pb_2La_2W_2Ti_4Nb_4O_{30}$ ferroelectric ceramic

L. Biswal · Piyush R. Das · Banarji Behera · R. N. P. Choudhury

Received: 14 November 2011 / Accepted: 1 October 2012 / Published online: 11 October 2012

Abstract A new single phase orthorhombic ferroelectric ceramic $Na_2Pb_2La_2W_2Ti_4Nb_4O_{30}$ (NPLWTN) was prepared via high-temperature solid-state reaction method. The grain morphology of the compound was analyzed by scanning electron microscopy (SEM). Studies of dielectric properties (ε_r and tanδ) of the compound at different frequencies (10^2–10^6 Hz) in a wide temperature range (300–700 K) showed multiple phase transitions in it. First phase transition observed at 335 K related to structural type (ferroelectric-ferroelectric) and the second one observed at 536 K is related to the ferroelectric to paraelectric. The ferroelectric property of the compound at room temperature was confirmed by polarization (hysteresis) study. Broadened dielectric peaks at low frequencies were observed above ferroelectric to paraelectric phase transition temperature (Tc). The values of exponent n(T) and pre-factor A(T) at and around Tc were obtained by the fitting ac conductivity data with Jonscher's universal power law. From the variation of n(T) and A(T) with temperature, the strength of interaction among the charge carriers with the crystal lattice and the strength of polarisability at phase transition are observed. The activation energy of the compound in low and high temperature range suggests the conduction mechanism in the material.

Keywords XRD · Diffused phase transition · Dielectric relaxation · AC conductivity

L. Biswal
Department of Physics, SOT, KIIT University,
Bhubaneswar 751024 Odisha, India

P. R. Das (✉) · R. N. P. Choudhury
Department of Physics, ITER, S. O. A. University,
Bhubaneswar 751030 Odisha, India
e-mail: prdas63@gmail.com
e-mail: prdas@iter.ac.in

L. Biswal · B. Behera
School of Physics, Sambalpur University,
Jyoti Vihar,
Burla 768019 Odisha, India

1 Introduction

There has been rapid progress in search of new ferroelectric materials for their industrial and commercial applications such as multi-layer capacitors, transducers, actuators, ferroelectric random access memory, electro-optic switches, pyroelectric detectors, optical modulators, mixers etc. [1–6]. Among all the known ferroelectric oxides of different structural families, some oxides of perovskite family have been found to be the most important one (economically). Even with some compromise on physical properties, now-a-days, few members of tungsten bronze (TB) structural family have been found promising candidates for wide spread technological applications. The tungsten bronze structure has an oxygen octahedral framework which is much more open than the simple perovskite structure (ABO_3 type). The basic unit cell of TB structures contains 10 BO_6 octahedral (corner-linked) to form square, triangular and pentagonal tunnels that extend through the structure along the 4-fold symmetry [7]. The c-axis linkage is regular, but in a and b directions the linkage is markedly puckered. There are two types of A sites (A_1, A_2) that can be occupied by large mono-valent, divalent, or trivalent ions. Two different B sites (B_1, B_2) that are usually occupied by smaller, highly charged cations (Nb, Ta, V, W, Ti), and C site being small, often remains vacant or occupied by Li, Er etc. [8–10]. Hence a general formula of tungsten bronze structure can be written as $[(A_1)_2(A_2)_4(C)_4][(B_1)_2(B_2)_8]O_{30}$. The properties of TB structured materials could vary a lot because of

the difference in their elements from the A to C sites, and are complicated due to their complex crystal structure. Thus a TB compound is a complex and disorder system, which is a derivative of perovskite structure. Detailed literature survey on the various properties and applications of TB structured compounds suggest that a lot of work have already been done except on titled compound. In view of the importance of the materials of the family, we have studied the structural, dielectric, and electrical properties of $Na_2Pb_2La_2W_2Ti_4Nb_4O_{30}$ (NPLWTN) and are reported here.

2 Experimental

2.1 Synthesis

The polycrystalline sample of the complex tungsten bronze niobate, $Na_2Pb_2La_2W_2Ti_4Nb_4O_{30}$ (abbreviated as NPLWTN), was prepared from high-purity (AR grade, ~99 % pure) raw materials; $NaCO_3$, PbO, La_2O_3, TiO_2, WO_3 and Nb_2O_5 (all from M/s Loba Chemical Co) using a high-temperature solid-state reaction technique. These ingredients (taken in a suitable stoichiometry) were thoroughly mixed and ground in dry (air) and wet (methanol) medium for 1 h each in an agate mortar. First, calcination was carried out in a high purity alumina crucible at 1273K for 4 h. The process of grinding and calcination was repeated twice to ensure the formation of the compound. The quality and formation of the compound were checked by preliminary X-ray structural analysis with diffraction data collected at room temperature (298 K) using X-ray powder diffractometer (PHILIPS PW1817) with CuKα radiation (λ=1.5418 Å) in a wide range of Bragg angles ($20^0 \leq 2\theta \leq 80^0$) at a scanning rate of 3 deg/min. The fine and homogenous powder was then cold pressed into pellets (10 mm diameter and 1–2 mm thickness) under a uni-axial pressure of $4\times10^6 N/m^2$ by a hydraulic press. Polyvinyl alcohol (PVA) was used as binder to reduce the brittleness of the pellets. Then the pellets were sintered for 4 h at 1,373 K in an air atmosphere. The binder was burnt out during the high temperature sintering process. After polishing(for making parallel surfaces), the pellets were electroded with high purity air-drying silver paste, and then dried at 423 K for 4 h, to remove moisture(if any) for electrical measurements. Microstructure of sintered pellet of the compound was recorded by JEOL JSM-5800 scanning electron microscope (SEM). The electrical measurements on a sintered pellet of the compound were carried out using a computer-controlled LCR meter (Hioki 3532) over a wide range of temperature. The room temperature hysteresis loop of the poled sample was obtained using precession material Analyzer (Radiant technologies Inc., USA) integrated with 4 kV voltage amplifier. The piezoelectric coefficients (d_{33}) of the compound was recorded on poled sample using piezometer (M/s. Piezo-test, Model: PM 200, UK).

3 Results and discussion

3.1 Structure/microstructure

Figure 1 shows the room temperature XRD pattern of NPLWTN. The XRD pattern suggests the formation of new compound [11]. Using the observed inter-planner spacing (d_{obs}) and 2θ of each peak of XRD pattern, unit cell parameters of the compound were obtained in different crystal systems and unit cell configuration with the help of a standard computer program package 'POWD' [12]. Finally, an orthorhombic unit cell was selected for the compound for which $\Sigma\Delta d = \Sigma (d_{obs} - d_{cal})$ was found to be minimum. The least-squares refined unit cell parameters are: a=17.6291(25) Å, b=18.7121(25) Å, c=3.8898(25) Å. These parameters are in agreement with similar compounds reported earlier [13].

Figure 1 (inset) shows the scanning electron micrograph of the compound. The texture and nature of micrograph confirmed the polycrystalline nature of the material. It was observed that the rod like grains of size in the range 2–13 μm are inhomogenously distributed over the entire surface of the sample with inter-grain porosity. A similar type of microstructure was observed in other crystalline materials of this family [6, 13]

3.2 Dielectric study

The variation of relative dielectric constant (ε_r) and loss tangent (tanδ) of the compound with frequency (10^2–10^6 Hz) at room temperature is shown in Fig. 2. It is observed that ε_r and tan δ decrease on increasing frequency showing a large dielectric dispersion in the low frequency region. This

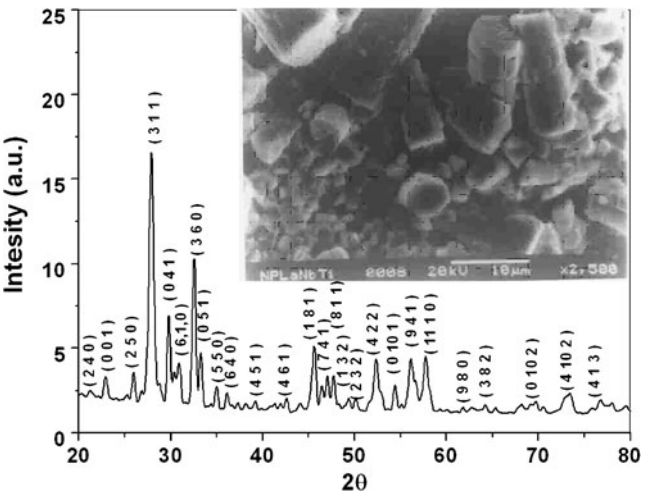

Fig. 1 Room temperature XRD pattern and SEM micrographs (inset) of $Na_2Pb_2La_2W_2Ti_4Nb_4O_{30}$

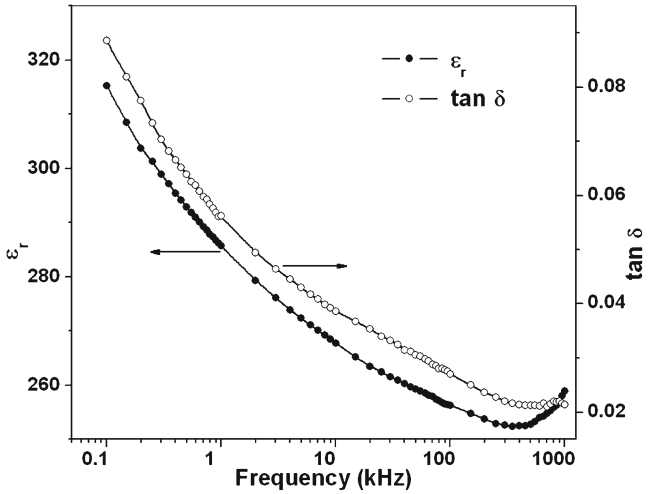

Fig. 2 Variation of ε_r and tanδ as a function of frequency at room temperature of $Na_2Pb_2La_2W_2Ti_4Nb_4O_{30}$

trend of a large dispersion at low frequencies is a common feature of polar dielectric materials with non negligible ionic conductivity, and is attributed to the low frequency space charge accumulation effect. This effect is considered as low frequency dielectric dispersion [14–17]. Also, the high value of dielectric constant of the studied compound at lower frequency is due to presence of all different type of polarizations (i.e., interfacial, atomic or ionic, dipolar and electronic) [18], but a larger contribution from space charge polarization. The space charge polarization effect decreases on increasing frequency. Therefore, the dielectric constant at higher frequencies is found to be smaller. It is clear that at higher frequency, the dielectric constant is less dispersive because of the major contribution to ε_r come from electronic polarization.

Figure 3 shows the temperature variation of ε_r and tanδ of the compound at frequencies 1, 10 and 100 kHz. Two

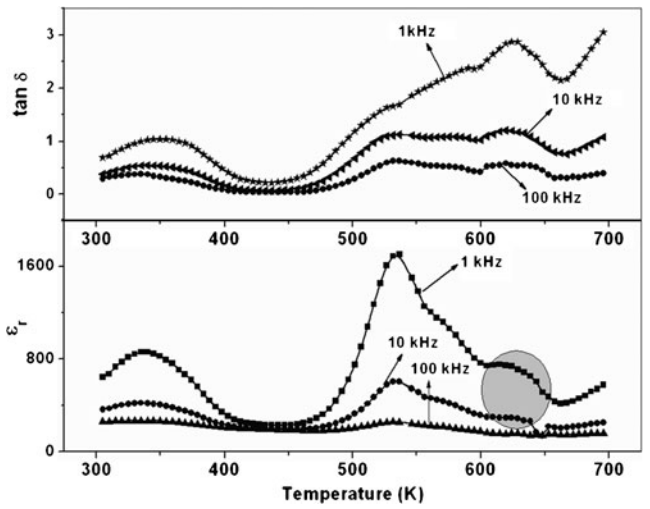

Fig. 3 Variation of ε_r and tanδ of $Na_2Pb_2La_2W_2Ti_4Nb_4O_{30}$ with temperature at 1 kHz, 10 kHz and 100 kHz

dielectric anomalies (at 335 K and 536 K) were observed for all the three frequencies. The value of ε_r increases gradually on increasing temperature and attains a maximum value (peak) at 335 K and then decreases. Once again, ε_r increases with increase in temperature and another peak is observed at 536 K. Further, on increasing the temperature ε_r increases rapidly. The rate of increase in ε_r (beyond second anomaly) at high temperature is again due to space charge polarization and comes from mobility of charge carriers and imperfections in the material. Such type of two phase transitions is reported earlier in many similar orthorhombic tungsten bronze ferroelectrics [19–21]. Based on this observations, it appears that the high temperature anomaly (536 K) is related to a ferroelectric—paraelectric transition (T_c), while the lower one (335 K) is related to structural type (ferroelectric—ferroelectric) transition. This conclusion is yet to be confirmed by suitable experiment. Therefore at this stage it is not possible to consider the type of phase transition including structural. The high temperature transition of the material was confirmed later by polarization study. In ε_r verses temperature graph, a dielectric dispersion was found in the paraelectric phase in low frequency region. At temperature 615 K, dielectric relaxation peak was observed. The dielectric relaxation peak may be the results of reorientation of off-centered Pb^{2+} and Nb^{5+} ions coupling. It is possible because of the presence of thermally activated conduction electrons appearing due to ionization of the oxygen vacancies. These electrons interact with the dipoles of the off-centered Pb^{2+} and Nb^{5+} ions and contribute to the dielectric relaxation peak [22, 23]. In the high frequency region (as the mobility of the charge carriers increases) the concentration of intrinsic oxygen vacancies and electrons become smaller and thus relaxation. The dielectric peak was found to be broadened indicating the existence of diffused phase transition. This broadening of dielectric peak can be attributed to structural disorder and compositional fluctuations in solid solution [24]. The degree of disorder (or diffusivity γ) in the compound is calculated using an expression $\ln(1/\varepsilon_r - 1/(\varepsilon_{r\,max})) = \ln K + \gamma \ln(T-T_c)$ [25], where K is an arbitrary constant. At 1 kHz, the value of γ was estimated from the slope of the curve, $\ln(1/\varepsilon_r - 1/\varepsilon_{r\,max})$ vs. $\ln(T-T_c)$ (Fig. 4). The calculated value of γ for the sample was found to be 1.26, which confirms the diffuse phase transition in the compound. It was observed that the compound has frequency independent transition temperature (no dielectric dispersion), which suggests that this compound does not have relaxor behavior. The maximum values of dielectric constant at T_c (ε_{max}) of the compound for 1, 10 and 100 kHz are 1,702, 603 and 255 respectively. The room temperature dielectric constants at 1, 10 and 100 kHz are 285, 267 and 258 respectively. Like dielectric constant multiple anomalies in loss tangent (Fig. 3) have been observed in the compound near to the transition temperatures

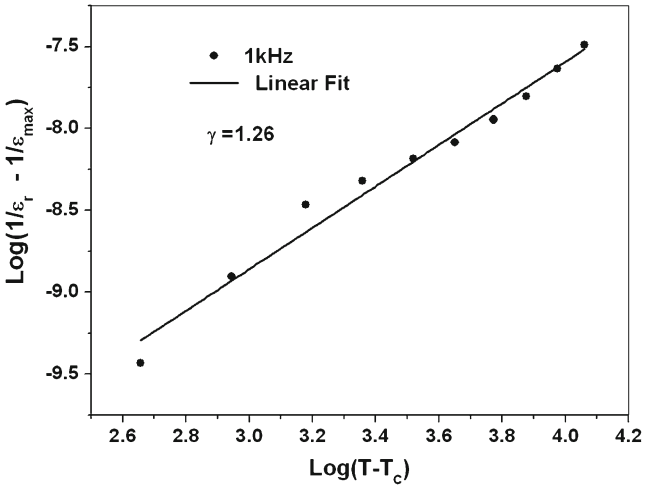

Fig. 4 Variation of ln $(1/\varepsilon_r - 1/(\varepsilon_{r\ max}))$ with ln $(T\text{-}T_c)$ for $Na_2Pb_2La_2W_2Ti_4Nb_4O_{30}$ at 1 kHz

because of the dynamics of domain-wall motion [24, 26]. Initially tanδ increases with temperature and then decreases near to transition temperature where the temperature changes the structure of the material,. This is a normal behavior of the ferroelectric materials [16]. In diffused phase transition, the dielectric constant and loss peaks occur at different temperatures with separation depending upon the degree of broadening of the peaks, and the temperature dependence of the dielectric relaxation [24]. The sharp increase in tanδ at high temperature is due to scattering of thermally activated charge carriers and defects in the sample. The behavior of tanδ at high temperature may be described by Arrhenius law especially at low frequencies. This suggests that the conduction mechanism at high temperature and low frequency is mainly due to thermal agitation. At higher temperature the conductivity begins to dominate, which in turn responsible for rise in tanδ. Also, at higher temperature the contribution of ferroelectric domain walls to tanδ decreases, which causes the rise in tanδ. The value of tanδ (at room temperature) is found to be 0.05, 0.03 and 0.02 at frequencies 1, 10 and 100 kHz respectively. In the low frequency region, a loss peak is observed near to 615 K which suggests the superimposition of relaxation and conductivity loss.

3.3 AC conductivity

Measurement of electrical conductivity was performed to understand the effect of conduction mechanism and the nature of the charge carriers in the material. The ac conductivity (σ_{ac}) of the sample was evaluated from the dielectric data using the relation: $\sigma_{ac}=\varepsilon_r\varepsilon_o\omega\ \tan\delta$, where ε_o is the vacuum dielectric constant and ω is the angular frequency. Jonscher [16] proposed a relation (usually referred as Jonscher's power law) to evaluate frequency dependence of dielectric materials:

$$\sigma_{ac}(\omega) = \sigma_{dc} + A\omega^n$$

Where, σ_{dc} is the frequency independent part of total conductivity. The coefficient A and exponent n are dependent on the material and temperature. The term $A\omega^n$ gives a measure of dispersion mechanism in conductivity. For $n<1$, the charge carriers are assumed to be taking a translational motion with sudden hoping [27], when $n>1$, suggests a localized hopping of the species with a small hopping without leaving the neighborhood [28].

Figure 5 shows the variation of electrical conductivity $\sigma_{ac}(\omega)$ with frequency at different high temperatures (in the paraelectric region). The conductivity is found to be increasing with increase in frequency and temperature. There is more dispersion in the low temperature than in the high temperature. As suggested, this may be due to electrode polarization. Again the conductivity is less at low frequencies because, at these frequencies, the mobility of charge carriers is less due to less concentration of oxygen vacancies. At high frequencies there is a tendency of merger of conductivity curves and hence dispersion becomes temperature and frequency independent. With increase in temperature, the conductivity response become more and more flattened in low frequency and high temperature regime which may be due to transition from long range hoping to short range ionic motion, and thus conductivity relaxation phenomena [23, 29] occurs. The ac conductivity with frequency graph is fitted with Jonscher's power law relation (Fig. 5). The value of σ_{dc} is obtained at different temperatures in the low frequency region. The variation of σ_{dc} with inverse of absolute temperature (in high temperature

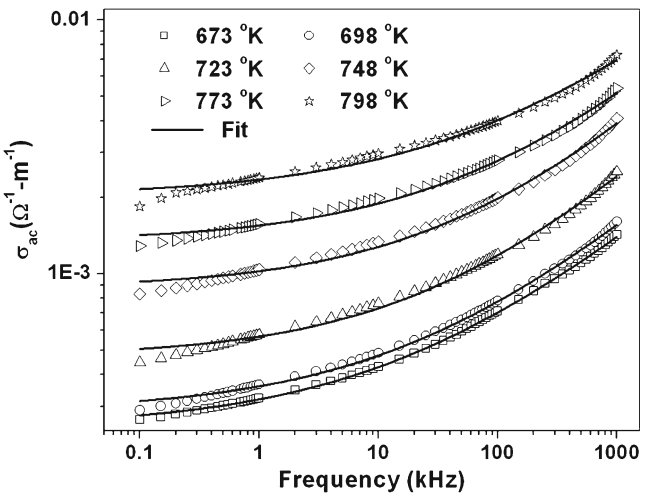

Fig. 5 Variation of ac conductivity (ln σ_{ac}) with frequency at different temperatures for $Na_2Pb_2La_2W_2Ti_4Nb_4O_{30}$. (Solid lines are fitted lines using Jonscher's power law)

regime) is shown in Fig. 6. The dc conductivity increases with increase in temperature, which exhibits negative temperature coefficient of resistance (NTCR). The activation energy at high temperature regime is calculated using Arrhenius plots (Fig. 6) and found to be 0.95 eV.

The temperature dependence of coefficient A and exponent n of Jonscher's power law is obtained from fitting of σ_{ac} with frequency graph (around ferroelectric transition temperature) The variation of n and A with temperature (calculated at high frequency regime) is shown in Fig. 7(a and b). The exponent n characterizes the interaction between the charge carriers participating in the polarization process. If the value of $n=1$, it is Debye type, which is attainable at very low temperature [14]. As the value of n decreases with rise in temperature in the ferroelectric region, it suggests the better interaction between the charge carriers. A minimum value of n at the transition temperature is observed. The value of n increases with further rise in temperature. The minimum value of n at T_c may be due to strong interaction between the charge carriers and the lattice [30]. The strength of polarisability (or non- ideal conductivity) is obtained from the critical value of coefficient A. For the studied sample it shows a peak at T_c. It arises from the diffusive motion of the carriers in phase transition region. It is argued that there exists a certain correlation between the dc conductivity and the non ideal conductivity, if both are due to the same charge carriers [31]

Figure 8 shows the temperature dependence of ac conductivity of the sample at 1 and 10 kHz. It is observed that the ac conductivity shows an anomaly in the vicinity of the dielectric peak corresponding to first anomaly. The ac conductivity peaks near the ferroelectric phase transition temperature occur due to the onset of large spontaneous polarization [32]. A linear variation of σ_{ac} over a wide temperature range (excepting at and near to the anomalies

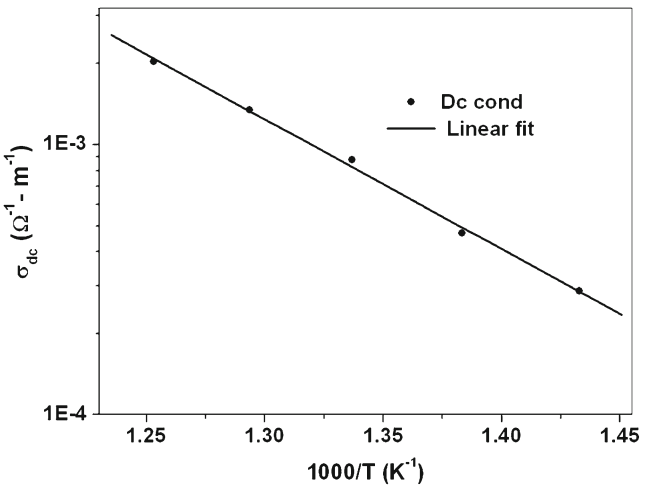

Fig. 6 Variation of dc conductivity (ln σ_{dc}) with temperature of $Na_2Pb_2La_2W_2Ti_4Nb_4O_{30}$

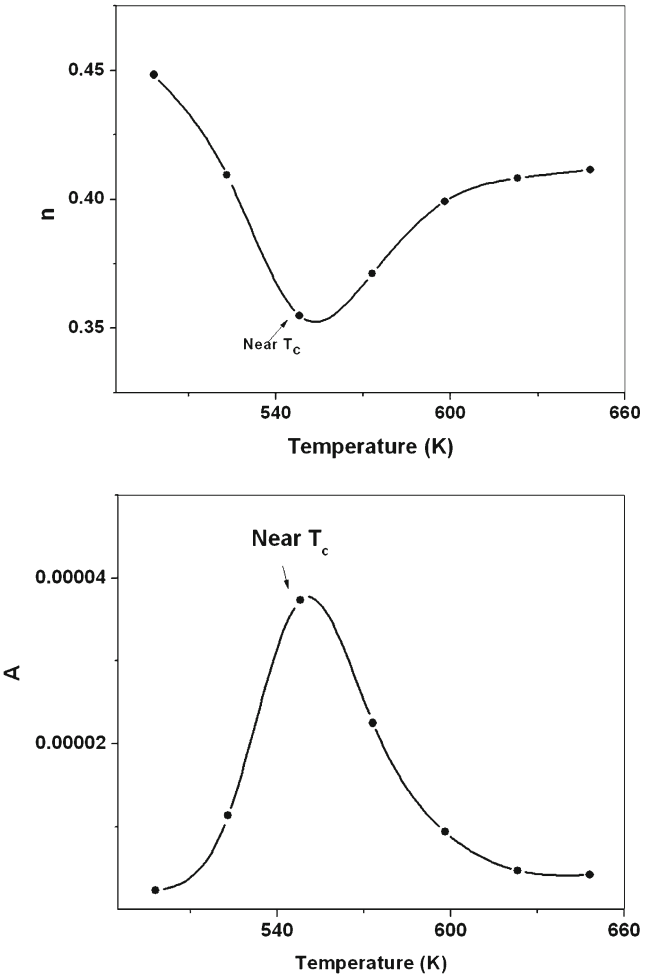

Fig. 7 (**a**) Variation of the exponent n with temperature near T_c for $Na_2Pb_2La_2W_2Ti_4Nb_4O_{30}$. (**b**) Variation of pre-factor A with temperature near T_c for $Na_2Pb_2La_2W_2Ti_4Nb_4O_{30}$

where there is an abrupt change in slope) supports the existence of thermally activated transport properties of the material which obeys the Arrhenius equation:

$$\sigma_{ac} = \sigma_o \exp(E_a/k_bT)$$

Where σ_o is the pre-exponential term, k_b is the Boltzmann constant and E_a is the activation energy. The value of the activation energy is obtained (using Arrhenius equation) in high temperature range from the slope of plot of 1000/T versus σ_{ac}. The value of E_a, calculated from the graph, was found to be 0.93 eV at 1 kHz and 0.80 eV at 10 kHz. The activation energy, calculated from dc conductivity graph in the same temperature range, is found to be 0.95 eV which is slightly higher than that of ac conductivity. Also, the value of activation energy calculated from ac conductivity graph at low frequencies is found to be more than at high frequencies. This is because at low frequencies, the conductivity is due to the mobility/transportation of charge carriers over long distances. On the other hand, at high frequencies,

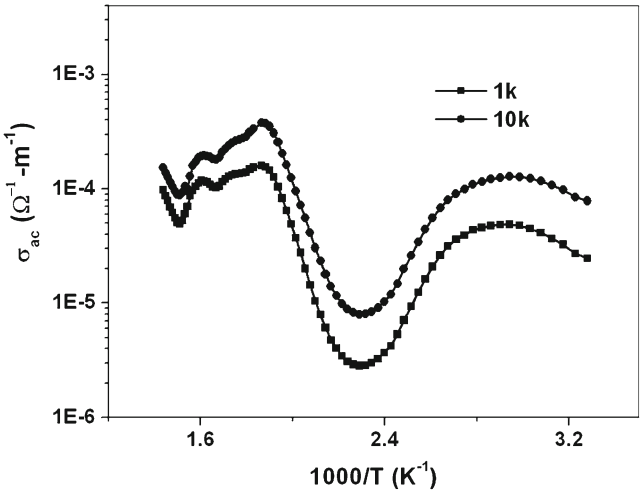

Fig. 8 Variation of ac conductivity (ln σ_{ac}) with temperature of $Na_2Pb_2La_2W_2Ti_4Nb_4O_{30}$ at 1 kHz and 10 kHz

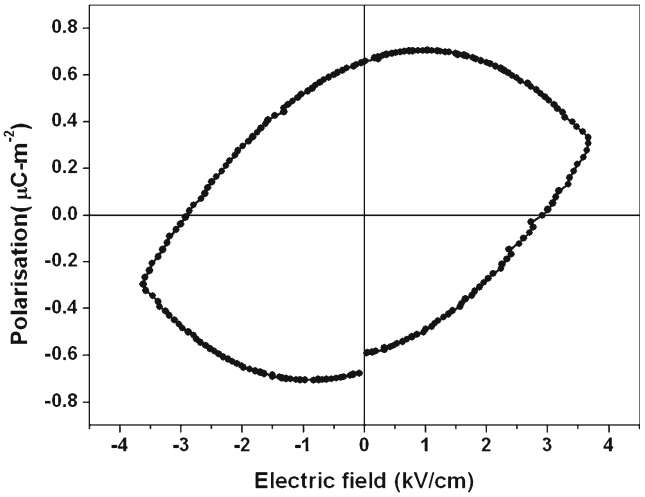

Fig. 9 P-E hysteresis loop of $Na_2Pb_2La_2W_2Ti_4Nb_4O_{30}$ at room temperature

because of relaxation/orientation mechanism, the charge mobility is restricted to the nearest neighboring lattice sites [23, 33]. Since the relaxation/orientation mechanism requires less energy than energy required for mobility of charge carriers over long distances, activation energy at high frequency is less than the activation energy for low frequencies. The values of activation energy E_a in low temperature range was found to be 0.20 eV at 1 kHz and 0.15 eV at 10 kHz. The magnitude of activation energy suggests the nature of charge carriers in the material. The value of E_a in the low temperature range is small. This may be due to the creation of large number of space charges and hopping of charge carriers (i.e., n and/or p-type [34]). The value of E_a in the high-temperature region is more than that of low temperature region; this is because of presence of small polarons [35, 36] and/or oxygen ions vacancies [34, 37]. The oxygen vacancies can create the electric dipoles which are responsible for the dielectric relaxation [22, 38]. It is seen that the value of activation energy depends on ionization level of the oxygen vacancy. Usually activation energy higher than 1.0 eV is connected to double ionized vacancies while those singly ionized ones have much smaller activation energy. Consequently, the conduction process within the high temperature range suggests the presence of singly ionized oxygen vacancies in the studied sample since the value of activation energy is found to be <1 eV. One may then conclude that the contribution to the conduction process in the material may be due to hoping of charge carriers at low temperatures and small polarons and/or singly ionized oxygen vacancies at high temperatures.

3.4 Polarization study

The hysteresis loop is one of the important measurements to characterize ferroelectric behavior of materials. Figure 9 shows the hysteresis loop of the poled sample at room temperature (at an applied field of 3.8 kV/cm). A gap in the loop and absence of saturation of polarization is observed owing to the maximum voltage (4 kV) of our experimental set up (Radiant Technologies Inc., USA). Similar type of lossy hysteresis loop in many tungsten bronze compounds has also been reported earlier [39]. The piezoelectric coefficient (d_{33}) of poled sample was found to be 5pC/N. This value of the compound was found to be very small as compared to other ferroelectric oxides (i.e., $BaTiO_3$, PZT, PLZT, PMN, etc.).

4 Conclusion

The polycrystalline sample of a new complex of tungsten bronze ceramic, $Na_2Pb_2La_2W_2Ti_4Nb_4O_{30}$, was prepared by a high-temperature solid-state reaction technique. X-ray diffraction structural analysis confirms an orthorhombic crystal structure of the compound at room temperature. The surface morphology of the sample, studied through SEM, gives various sizes of grains ranging from 2 to 13 μm. The SEM micrograph further shows that the grains are in-homogenously distributed over the surface of the sample. Two dielectric anomalies at 335 K and 536 K may be associated with structural and ferroelectric-paraelectric transition of diffused type respectively. The ε_r versus temperature graph showed dielectric relaxation at 615 K in low frequency region. Temperature dependence of the exponent n(T)) and the strength of the polarisability A(T)) are determined using Jonscher's power law. The minimum value of n at T_c is due to the strong interaction between the charge carriers and the lattice. The pre-factor A(T), which arises due to the diffusive motion of charge carriers, shows a peak at T_c. The dispersion in ac conductivity at low frequencies is due to the electrode

polarization. The activation energy at high temperature calculated from dc conductivity (i.e. 0.95 eV) is more than the ac conductivity (i.e. 0.93 eV at 1 kHz and 0.80 eV at 10 kHz). Conduction process in the material may be due to hoping of charge carriers at low temperatures and small polarons and/or singly ionized oxygen vacancies at high temperatures.

Acknowledgments One of the authors (BB) acknowledges the financial support through DRS-I of UGC under SAP for the development of research work in the School of Physics, Sambalpur University.

References

1. K. Uchino, *Ferroelectrics devices* (Marcel Dekker, New York, 2000)
2. O. Auciello, J.F. Scott, R. Ramesh, Phys. Today **51**, 22 (1998)
3. T.M. Herbert, *Ceramic dielectrics and capacitors* (Gordon and Breach Science Publishers, New York, 1985)
4. R.R. Neurgaonkar, J.R. Oliver, L.E. Cross, Ferroelectrics **56**, 1035 (1984)
5. B. Behera, P. Nayak, R.N.P. Choudhary, Mater. Chem. Phys. **100**, 138 (2006)
6. P.R. Das, L. Biswal, B. Behera, R.N.P. Choudhary, Mater. Res. Bull. **44**, 1214 (2009)
7. P.B. Jamieson, S.C. Abrahams, J.L. Bernstein, J. Chem. Phys. **48**, 5048 (1968)
8. S.C. Abrahams, P.B. Jamieson, J.L. Bernstein, J. Chem. Phys. **54**, 2355 (1971)
9. L.G. VanUitert et al., Mater. Res. Bull. **3**(47) (1968)
10. B.A. Scott et al., Mater. Res. Bull. **5**(47) (1970)
11. H.P. Klug, L.E. Alexander, *X-ray diffraction procedures* (Wiley, Chichester Engl, 1974)
12. E. Wu, *POWD, An Interactive Powder Diffraction Data Interpretation and Indexing Program*, Ver. 2.1, School of Physical Sciences, Flinders University South Bedford Park, SA 5042, Australia
13. P.R. Das, R.N.P. Choudhary, B.K. Samantray, Mater. Chem. Phys. **101**, 228 (2007)
14. Z. Lu, J.P. Bonnet, J. Ravez, P. Hagenmuller, Solid State Ionics **57**, 235 (1992)
15. T.A. Nealon, Ferroelectrics **76**, 377 (1987)
16. A.K. Jonscher, *Dielectric relaxation in solids* (Chelsea Press, London, 1983)
17. A.K. Jonscher, R.M. Hill, C. Pickup, J. Mater. Sci. **20**, 4431 (1985)
18. K. Chi Kao, *Dielectric phenomena in solids* (Elsevier Academic Press, Amsterdam, 2004)
19. R.J. Xie, Y. Akimune, K. Matsuo, T. Sugiyama, N. Hirosaki, T. Sekiya, Appl. Phys. Lett. **80**, 835 (2002)
20. L. Fang, H. Zhang, B. Wu, R. Yuan, Pro. Cryst. Gro. Charact. Mater. **40**, 161 (2000)
21. B. Behera, P. Nayak, R.N.P. Choudhary, J. Phy. Chem. Solids **69** (1990) (2008)
22. C. Ang, Z. Yu, L.E. Cross, Phy. Rev. B **62**, 228 (2000)
23. K. Sambasiva Rao, P. Murali Krishna, D. Madhava Prasad, J.-H. Lee, J.-S. Kim, J. Alloys Comp. **464**, 497 (2008)
24. M.E. Lines, A.M. Glass, *Principles and applications of ferroelectrics and related materials* (Oxford University Press, London, 1977)
25. S.M. Pilgrim, A.E. Sutherland, S.R. Winzer, J. Am. Ceram. Soc. **73**, 3122 (1990)
26. I.S. Zheludev, *Physics of crystalline dielectrics*, vol. 2 (Plenum Press, New York, 1971)
27. K. Funke, Prog. Solid State Chem. **22**, 111 (1993)
28. S. Sen, R.N.P. Choudhary, Mater. Chem. Phys. **87**, 256 (2004)
29. R. Mizaras, M. Takasighe, J. Banys, S. Kojima, J. Grigas, S.I. Hamazaki, A. Brilingas, J. Phys. Soc. Jpn. **66**, 2881 (1997)
30. D.M. Ginsberg (ed.), *Physical properties of high temperature super conductors I and II* (World Scientific, Singapore, 1989)
31. A.E. Paladino, J. Am. Ceram. Soc. **48**, 476 (1965)
32. J.R. Oliver, R.R. Neurgaonkar, L.E. Cross, J. Appl. Phys. **64**(1), 37 (1988)
33. S. Mahaboob, G. Prasdand, G.S. Kumar, Bull. Mater. Sci. **29**, 35 (2006)
34. N.V. Prasad, G. Prasad, T. Bhimasankaram, S.V. Suryanarayana, G.S. Kumar et al., Bull. Mater. Sci. **24**(487) (2001)
35. K.K. Patanker, V.L. Mathe, A.N. Patil, S.A. Patil, S.D. Lotke, Y.D. Kolekar, P.B. Joshi, J. Electroceram. **6**, 115 (2001)
36. E.A. Kotomin, R.I. Egilitis, G. Borstel, J. Phys. Condens. Mater. **12**, L557 (2000)
37. F.D. Morrison, D.C. Sinclair, A.R. West, J. Appl. Phys. **86**, 6355 (1999)
38. B.S. Kang, S.K. Choi, C.H. Park, J. Appl. Phys. **94**, 1904 (2003)
39. P.S. Das, P.K. Chakraborty, B. Behera, R.N.P. Choudhary, Physica B **395**, 98 (2007)